Journal Pre-proofs

Fatigue Cracking Characterisations of Waste-derived Bitumen Based on Crack Length

Linglin Li, Yangming Gao, Yuqing Zhang

PII: S0142-1123(20)30506-5
DOI: https://doi.org/10.1016/j.ijfatigue.2020.105974
Reference: JIJF 105974

To appear in: *International Journal of Fatigue*

Received Date: 23 June 2020
Revised Date: 24 September 2020
Accepted Date: 28 September 2020

Please cite this article as: Li, L., Gao, Y., Zhang, Y., Fatigue Cracking Characterisations of Waste-derived Bitumen Based on Crack Length, *International Journal of Fatigue* (2020), doi: https://doi.org/10.1016/j.ijfatigue.2020.105974

Fatigue Cracking Characterisations of Waste-derived Bitumen Based on Crack Length

Linglin Li [a, b] Yangming Gao [b] and Yuqing Zhang [b, *]

[a] School of Automotive & Transportation Engineering, Hefei University of Technology, Hefei, China

[b] Aston Institute of Materials Research, Aston University, Birmingham, United Kingdom

Abstract: This study aims to characterise fatigue cracking of two types of waste-derived (bio-oil and LDPE) bitumen. Modified Paris' law and Griffith criterion were proposed to investigate crack propagation and initiation of the bitumen. Results show that the bio-oil delays and the LDPE accelerates crack initiation, and the bitumen itself dominates crack propagation of unaged bitumen. The bio-oil did not take the effects in altering bitumen's fatigue performance after pressure ageing vessel (PAV) ageing. PAV-aged LDPE modified bitumen is more prone to fatigue crack in crack initiation phase, but it remains the same crack propagation rate as PAV-aged control bitumen.

Keywords: Waste-derived Bitumen, Ageing, Fatigue Cracking, Bio-oil, Plastics

* Corresponding author.
E-mail address: l.li28@aston.ac.uk (Linglin Li), gaoy14@aston.ac.uk (Yangming Gao), y.zhang10@aston.ac.uk (Yuqing Zhang)

1. Introduction

Petroleum-derived bitumen is a by-product of crude oil distillation and heavily used as a binder for transport infrastructures, e.g., surface paving of roads [1], highways [2], bridges [3], car parks [4] and airport runways [5]. However, over the years there have been increased concerns over negative environmental effects of petroleum industry [6]. Moreover, from the perspective of economic evaluation, the bitumen accounts for approximately 40~50% of the cost of materials used to produce asphalt mixture. Consequently, the cost of asphalt mixture is very sensitive to the price of the bitumen, which is then related to the price of crude oil in most cases. Therefore, it is essential that the eco- and cost-friendly bitumen is sought.

Meanwhile, in the UK there are nearly 8 million tonnes of household waste plastics and municipal solid waste (MSW) almost unrecycled and typically landfilled or incinerated each year. One of the most promising methods to recycle a certain portion of these wastes is to use them as construction materials for transport infrastructures [7, 8]. Regarding the waste plastics, laboratory experiments show that incorporating waste plastics (by 5~10wt.%) into asphalt mixture can effectively enhance its stability [9], strength [10], and durability [11]. At present, there are mainly two options for recycling waste plastics in asphalt mixture, namely, the dry way to replace fine aggregate [12] and the wet way to serve as a binder modifier [8]. In terms of the MSW, originally collected from households and then processed at Material Recovery Facilities for recovering recyclable materials, the main components are decomposed food, papers, textiles, plastics, wood, and some inert materials. Hence, it is not feasible to directly use them without proper processing to enhance the eco, cost or mechanical performance of the bitumen or asphalt mixture. Recently, pyrolysis, which is a thermochemical decomposition of organic material that occurs at moderate temperatures of 300~500°C in the absence of oxygen, has been employed as a method for waste disposal and energy recovery [13]. There have been increasing research activities and industrial developments of pyrolysis of the MSW by using a different type of reactors to produce pyrolysis oil [14]. In addition, duo to its great application potential showed by the altered physical, chemical, mechanical and economical properties [7, 13], pyrolysis oil derived from the MSW has attracted increasing research attention and been regarded as a promising candidate to enhance the bitumen's engineering performance. However, an increasing demand is substantially raised for a comprehensive understanding and an accurate prediction of engineering performance (e.g., fatigue) of the bitumen modified by those waste materials including the waste plastics and MSW pyrolysis liquid.

It is observed that fatigue crack is one of the most common distresses caused by load-induced deterioration in asphalt pavements at intermediate temperatures (e.g., 20°C) [15]. The fatigue performances (e.g., fatigue life) of asphalt pavement are dependent of fundamental material properties (e.g., shear relaxation modulus, shear strength and receding surface energy) of the bitumen, which contribute to the microcrack initiation [16], propagation [17], and ultimately coalescence of microcracks and growth in the form of macrocracks [18] in the asphalt pavement. Damadi et al. [19] investigated fatigue performance of the bitumen modified by composite of Nano-SiO_2 and Styrene Butadiene Styrene (SBS) Polymer, and concluded that this new component Nano-SiO_2 can mitigate the phase separation of SBS modified bitumen and improve its potential of fatigue failure resistance. Ameri et al. [20] evaluated fatigue property of reclaimed asphalt binder (RAB) modified with rejuvenator and softer bitumen. They found that both the rejuvenator and softer bitumen can effectively enhance the fatigue performance of the bitumen containing up to 100% RAB and 50% RAB in the virgin bitumen, respectively. Although there were lots of other research efforts [21-23] on fatigue properties of the modified bitumen, but how the fatigue performance alters when the bitumen

is modified with the waste plastics and MSW is still unknown. Hence, accurate characterisation and quantification of fatigue properties of the novel bitumen derived from the waste plastics and MSW are important for performance optimisation and evaluation of extension of their service life.

Until recent, how to select proper material parameters to characterise fatigue cracking performance has attracted more attentions. To characterise fatigue cracking of the bitumen, fatigue index, defined by the product of dynamic shear modulus and sine values of phase angle, was firstly developed by the Strategic Highway Research Program (SHRP) to quantify fatigue performance of the bitumen at intermediate temperature [24]. However, many recent research efforts showed that there were poor correlations between this fatigue index and the fatigue performance of asphalt mixture produced with modified bitumen [25-28]. Continuous efforts were made to search for alternative test methods to correlate fatigue performance of the bitumen well with the one of asphalt pavements, which mainly consisted of time sweep test and linear amplitude sweep (LAS) test. Anderson et al. [29] firstly reported that in time sweep test the curve of dynamic modulus versus load cycle presented a typical fatigue behaviour, based on which they recommended that time sweep test can be selected as a bitumen specification for the characterisation of fatigue cracking. The other well-known test method is LAS, which was proposed based on viscoelastic continuum damage (VECD) theory [30]. In the time sweep and LAS tests, the widely used fatigue parameters were dissipated strain energy [31], dissipated pseudo strain energy [32], pseudo stiffness [33], and internal state variable [34], all of which were indirect and empirical indicators for defining fatigue cracking of the bitumen. Zhang and Gao [35] successfully developed a damage mechanics-based crack growth model (i.e., dynamic shear remoter-cracking (DSR-C) model) and used crack length to characterise fatigue cracking performance of the bitumen based on the time sweep test. Integrated with the modified Paris' law and Griffith criterion, this paper is going to present both crack propagation and initiation behaviour of the bitumen, the benefit of which is that only fundamental material constants (e.g., shear relaxation modulus, shear strength and receding surface energy) are needed to serve as an evaluation of the resistance to fatigue cracking of the waste-derived bitumen.

This study aims to characterise fatigue cracking performance of two types of waste-derived bitumen, including the bio-oil modified bitumen using MSW pyrolysis liquid and the plastic modified bitumen by low-density polyethylene (LDPE). Theoretical fatigue cracking models of the bitumen based on the DSR tests were firstly presented, followed by the DSR fatigue tests and surface energy experiments. This consisted of the fabrications of the bio-oil modified bitumen and the LDPE modified bitumen, preparation of the DSR and surface energy specimens, and receding contact angle tests of virgin and PAV-aged waste-derived bitumen. Then, characterisations of cracking performances of virgin and PAV-aged control and waste-derived bitumen were analysed in detail, based on which how the waste materials affected crack initiation and propagation were quantified. Last section summarised the main contributions of this paper.

2. Theoretical Models for Bitumen Cracking

2.1 Crack Propagation and Initiation of Bitumen under a Rotational Fatigue Load

Dynamic shear rheometer (DSR) is commonly utilised to characterise the viscoelastic properties of the bitumen; additionally, it can be effectively used to evaluate and predict the fatigue crack performance of the bitumen by applying a rotational fatigue load. Zhang and Gao [35] proposed a damage mechanics-based crack growth model, which was employed to calculate the crack length of the bitumen under the rotational shear fatigue load. The crack

length in a strain controlled DSR time sweep fatigue test can be shown by **Equation (1)**:

$$CL = \left\{1 - \left[\frac{\left|G_N^*\right| / \sin\left(\delta_N\right)}{\left|G_0^*\right| / \sin\left(\delta_0\right)}\right]^{1/4}\right\} r_0 \tag{1}$$

Where, CL is the crack length of the bitumen at the N^{th} load cycle; $|G^*_0|$ and δ_0 are the dynamic shear modulus and phase angle of the bitumen in the undamaged state, respectively; $|G^*_N|$ and δ_N are the dynamic shear modulus and phase angle of the bitumen at the N^{th} load cycle in the damaged state, respectively; r_0 is the original radius of the bitumen sample (i.e., 4mm in this study).

Equation (1) presents an accurate and effective method to calculate crack length of the bitumen in a time sweep procedure of the DSR test using measured shear modulus and phase angle. It should be noted that the $|G^*_0|$ and δ_0 can be calibrated at relatively low strain level (e.g., 0.1%-0.5%) and intermediate temperatures (e.g., 15°C and 20°C) of a linear amplitude sweep procedure; the $|G^*_N|$ and δ_N can be measured at high amplitudes of shear strain (e.g., 5% and 7%) of the time sweep procedures (e.g., 15 and 20°C; 10 and 20Hz). The damaged bitumen samples after the time sweep procedures were firstly cooled down to 3°C followed by their uninstallations. Then, digital visualisations of cracked surfaces for two types of neat bitumen, one polymer-modified bitumen, and two types of waste-derived bitumen before and after ageing was conducted to obtain the measured values of crack lengths. Results show that **Equation (1)** can accurately predict the crack length in different types of bitumen (neat bitumen, polymer modified bitumen, and waste-derived bitumen) before and after ageing. Part of these results can be found the authors' published paper [35].

The original Paris' law is a crack growth equation that gives the rate of a fatigue crack growth of a linear elastic material [36]. Lytton et al. [37] extended the application of original Paris' law to viscoelastic media (e.g., asphalt) by employing the pseudo parameters (e.g., pseudo *J*-integral and pseudo strain energy release rate), which were originally proposed by Schapery [38]. Using the crack length to characterise the fatigue cracking, the modified Paris' law can be presented by **Equation (2)**:

$$\frac{dCL}{dN} = A\left(\Delta J_R\right)^n \tag{2}$$

Where, N is load cycle; A and n are crack related material constants; ΔJ_R is the incremental pseudo *J*-integral, which can be calculated by **Equation (3)** for a strain controlled rotational shear fatigue load, e.g., in time sweep test [39]:

$$\Delta J_R = \frac{\pi}{2}\frac{\left|G_0^*\right|}{G_R}\left|G_N^*\right|\frac{\left(r_E^{N-1}\theta\right)^2}{h}\sin\left(\delta_N - \delta_0\right) \tag{3}$$

Where, G_R is the shear reference modulus and assigned to the dynamic shear modulus $|G^*_0|$ [40]; r_E^{N-1} is the uncracked radius of the DSR sample at the $(N\text{-}1)^{th}$ load cycle, and it can be determined as $r_E^{N-1} = r_0 - CL^{N-1}$ where CL^{N-1} can be determined by **Equation (1)**; θ is the amplitude of rotational angle controlled by DSR; h is the height of the DSR sample.

It is worth noting that the incremental pseudo J-integral in **Equation (3)** mitigates the viscous impact on the crack growth of the bitumen and quantifies the pseudo strain energy release rate duo to crack growth. It also should be stressed that the modified Paris's law only can be

used for the characterisation of crack propagation; hence, the $|G^*_N|$, δ_N, and r_E^{N-1} should be obtained at the crack propagation phase in the crack curve. Additionally, **Equation (3)** has been successfully employed to interpret the "shallow" and "deep" crack growths of crack propagation, details of which can be found in the authors' recent work [39].

Schapery [41] proposed theoretical models to calculate A and n of the polymer based on its fundamental material parameters, which can be shown in **Equations (4)** and **(5)**.

$$A = \frac{1}{\tau_m^2}\left[\frac{\sin\left(m'\pi\right)}{\pi m' G_1}\right]\left(\frac{G_R}{\Delta G_f}\right)^{2n} \tag{4}$$

$$n = \frac{1}{m'} \tag{5}$$

Where, τ_m is the shear strength; m' is the slope of double logarithmic shear relaxation modulus curve; G_1 is the initial shear relaxation modulus, where the shear relaxation modulus is modelled as $G(t) = G_1 t^{-m'}$; and ΔG_f is the fracture bond energy that is two times of its surface energy calculated from the receding contact angles.

Griffith [42] stated that a critical condition for crack initiation was that the total external energy input was equal to the energy consumed in creating new cracked surfaces. Combined with the correspondence principle proposed by Schapery [38], Griffith criterion when applied to the bitumen can be expressed as follows:

$$\frac{\partial W^R}{\partial CL} = 0 \tag{6}$$

Where, W^R is the total pseudo strain energy after the energy redistribution in the DSR bitumen sample, which can be formulated by **Equation (7)**:

$$W^R = \int_{V_{total}} RPSEdV_{total} - \int_{V_{crack}} RPSEdV_{crack} + \Gamma_f \cdot (C.S.A) \tag{7}$$

Where, *RPSE* is the recovered pseudo strain energy; Γ_f is the surface energy calculated from the receding contact angles; *C.S.A* is the crack surface areas including the upper and lower crack surfaces; and V_{total} and V_{crack} are the total and cracked volume of DSR bitumen sample, respectively. Details of **Equation (7)** can be found in the Appendix of this paper.

Hence, the crack initiation criterion of the bitumen in a strain controlled time sweep fatigue test can be obtained by substituting **Equation (7)** into **Equation (6)**, and the critical strain level at which the crack is initiated can be calculated by:

$$\gamma_{0initiate} = \frac{\theta}{h} CL_0 + \frac{2}{\left|G_0^*\right|}\left(\frac{G_R}{h}\Gamma_f\right)^{1/2} \tag{8}$$

Where, $\gamma_{0initiate}$ is the critical strain for crack initiation; and CL_0 is the "edge-flow" crack length for crack initiation of the DSR bitumen sample [43]. Detail of the derivation of **Equation (8)** can be found in the Appendix of this paper. It is also noted that **Equation (8)** is a reformed model for the critical strain at cracking initiation that was derived as **Equation (21)** in the authors' recent work [43] where a relationship between film thickness (h) and the energy release area (ka) is used as $h = ka$.

2.2 Calculation of Surface Energy of Bitumen

Surface energy Γ is one of the key parameters affecting the cracking properties of the bitumen. However, it is not feasible to directly measure it, and at present one of the preferred methods is to measure contact angles using sessile drop method and then determine the surface energy of the material. In this method, the drops of a small amount of probe liquids are deposited on the bitumen sample surface and the contact angles between the liquids and the bitumen surface are measured, based on which the surface energy can be obtained using Young-Dupre equation [44]:

$$\left(1+\cos\theta\right)\Gamma_{liquid} = 2\left[\sqrt{\Gamma^{LW}\Gamma^{LW}_{liquid}} + \sqrt{\Gamma^{+}\Gamma^{-}_{liquid}} + \sqrt{\Gamma^{-}\Gamma^{+}_{liquid}}\right] \quad (9)$$

Where, θ is contact angle between the probe liquid drop and the bitumen; Γ_{liquid}, Γ^{LW}, Γ^{LW}_{liquid}, Γ^{+}, Γ^{-}, Γ^{+}_{liquid}, and Γ^{-}_{liquid} are the surface energy of the probe liquid, the Lifshitz-van der Waals component of the bitumen, the Lifshitz-van der Waals component of the probe liquid, the Lewis acid component of the bitumen, the Lewis base component of the bitumen, the Lewis acid component of the probe liquid, and the Lewis base component of the probe liquid, respectively.

After obtaining the values of Γ^{LW}, Γ^{+}, and Γ^{-}, the total surface energy can be calculated by:

$$\Gamma = \Gamma^{LW} + 2\sqrt{\Gamma^{+}\Gamma^{-}} \quad (10)$$

3. Materials and Experimental Characterisation

3.1 Fabrication of Waste-derived Bitumen

Bitumen X70 was selected as a control and base bitumen to develop the waste-derived bitumen by mixing with waste material (i.e., bio-oil or LDPE). The concentrations of bio-oil and LDPE in the modified bitumen were 5wt. % and 6wt. %, respectively. Detailed characterisations of the control bitumen, bio-oil, and LDPE can be found in **Table 1**.

Table 1. Characterisations of X70, bio-oil, and LDPE

		Measure	Value
X70 [a]	Penetration @25°C	dmm	45-80
	Softening Point	°C	≥45
	Force Ductility @5°C	J/cm^2	>3
	Flash Point (Cleveland)	°C	>250
	Fraas Breaking Point	°C	≤-12
bio-oil [b]	Water Content	wt. %	25.4
	Solid Content	wt. %	19.3
	Higher Heating Value	MJ/kg	28.0
	Density	g/cm^3	0.972
LDPE [c]	Melting Point	°C	126
	Melting Heat	MJ/kg	0.141
	Density	g/cm^3	0.934
	Thermal Degradation Point	°C	220

[a] Data provided by the supplier. [b] Data referenced from the authors' previous work [13]. [c] Data obtained from DSC and density tests.

To fabricate 5wt. % bio-oil modified bitumen, bio-oil was firstly put into a clean beaker

followed by adding well-calculated mass of hot control bitumen. Then, a high shear mixer is used to mix them homogenously at a speed of 150RPM for 30min at 150°C under nitrogen atmosphere. Regarding the 6wt. % LDPE modified bitumen, hot control bitumen was firstly put into another clean beaker followed by adding accurately calculated mass of the LDPE. Then, the high shear mixer is utilised to blend the LDPE at a speed of 900RPM for 90min at 180°C under nitrogen atmosphere. The blending speed and time were selected to ensure the LDPE was completely melted and distributed within the hot bitumen.

3.2 Preparation of DSR and Surface Energy Test Specimens

As mentioned in Section 2, the designed tests mainly include DSR tests and surface energy tests. The major goal of the DSR tests is to accurately measure shear strengths, dynamic moduli, and phase angles of the undamaged and damaged bitumen. In terms of surface energy tests, the main objective is to obtain contact angles between the bitumen and probe liquids.

Before starting the tests, the bitumen samples stored in containers were heated in laboratory oven at 165°C for 30min to reduce material viscosity. Then hot bitumen was carefully distributed into silicone specimen mold with a cavity of 8mm in diameter and 2 mm in depth. After 15 minutes, the DSR sample was carefully demoulded from the mold and be installed and trimmed on the surfaces of bottom and top plates to conduct the DSR tests shown in **Figure 1**. The LAS, frequency sweep and fatigue tests were conducted on the DSR using an 8 mm diameter parallel plate geometry and 2 mm gap setting, as shown in **Figure 1**. To make the bitumen samples contact well with the DSR plates and reduce the heterogeneity due to the fabrications of these samples, all bitumen samples were preheated to 80°C before the tests started. After the DSR tests, both plates were checked carefully to make sure the adhesions between them were still excellent. To examine the repeatability of the experiments, three replicates were tested at each condition and additional replicates were added when the repeatability COV of target shear strengths, dynamic moduli and phase angles were greater than 5%, 10%, and 5%, respectively, which is in consistent with the standard of EN 14770: 2012.

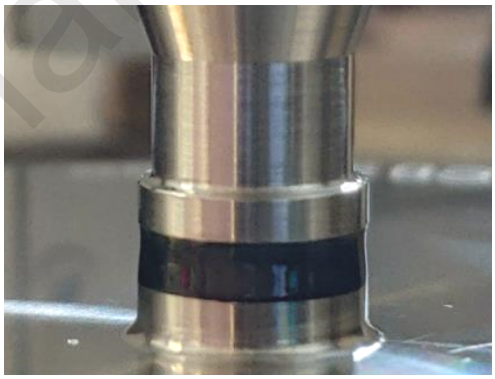

Figure 1. Trimmed configuration of an undamaged cylindrical bitumen sample

In this paper, surface energy for cracking was measured by a versatile optical tensiometer, where the Attension Theta Flex tensiometer was used. Microscope slides with 76 × 26 ×1mm dimensions were cleaned by acetone and distilled water, and then dried by laboratory oven at 60°C for 30min. After that, the slides were dipped into the melted bitumen for 10 seconds and then held out of the container for another 10 seconds to make extra hot bitumen drop off the slide. To get a flat and smooth surface of the bitumen sample, the above process needs repeating for at least 3 times, if necessary. Then the bitumen sample was cooled to ambient temperature in a desiccator with anhydrous calcium sulphate crystals for 24 hours. **Figure 2**

presents the bitumen in the container and on microscope slides, and the installation of microscope slide coated with the bitumen on the Attension Theta Flex tensiometer.

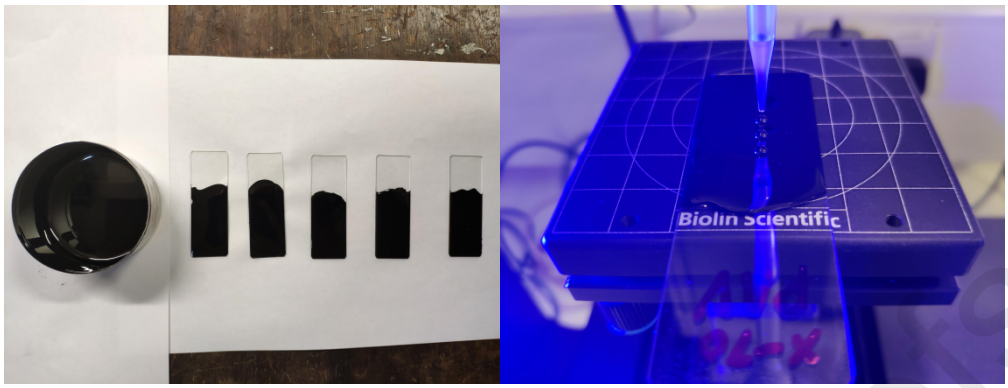

Figure 2. Bitumen in container and on microscope slides, and contact angle test of the bitumen by Attension Theta Flex tensiometer

3.3 Experimental Characterisation of Bitumen

a) LAS test to determine shear strength, dynamic shear modulus and phase angle

To calculate crack length, incremental pseudo *J*-integral and material parameters (*A* and *n*) described in Section 2, shear strength, dynamic shear modulus and phase angle of the undamaged bitumen need to be calibrated firstly. **Figure 3** presents the stress and strain relationship obtained from linear amplitude sweep (LAS) test of the unaged control bitumen conducted at 10Hz and 20°C. In the LAS test, the start and end shear strain level were selected as 0.01% and 100%, respectively. As described by AASHTO TP 101-14 [45], the LAS test can be used to evaluate the ability of the bitumen to resist shear damage by employing cyclic shear loading at increasing amplitude to accelerate damage. Hence, shear strength of the bitumen is the peak stress value τ_m (i.e., 290.4 kPa for this unaged control bitumen) based on the curve of shear stress versus shear strain.

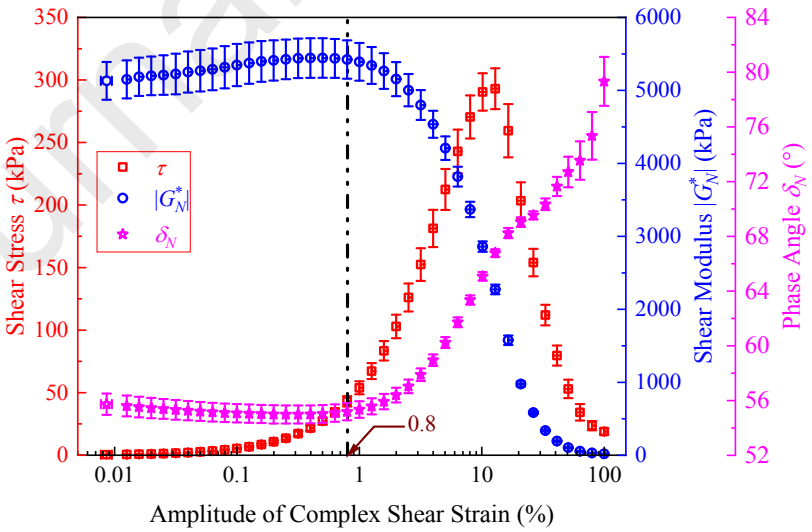

Figure 3. Dynamic shear modulus, phase angle and shear stress versus strain curves from LAS test (10Hz and 20°C)

Figure 3 also shows that, in the LAS test, both dynamic shear modulus and phase angle vary little or remain the same when the amplitude of shear strain is low, e.g. less than 0.8%. This implies that 0.8% is a critical threshold strain level, below which the selected unaged control

bitumen sample is undamaged at 10Hz and 20°C. When the amplitude of shear strain is over 0.8%, dynamic shear modulus decreases and phase angle increases dramatically, which indicates that cracks appear in the control bitumen. Theoretically, the $|G^*_0|$ and δ_0 can be obtained by averaging the $|G^*_N|$ and δ_N in a strain level between 0.01% and 0.8%, within which the bitumen is in an undamaged condition. But practically, the sample-to-sample variation of the bitumen needs to be considered, because the $|G^*_0|$ and δ_0 measured herein will be used to characterise the fatigue performance of the bitumen by integrating the following results of frequency sweep tests and fatigue tests. The DSR bitumen sample after the LAS tests which is already damaged cannot be reused to investigate fatigue properties of the unaged control bitumen. Therefore, a new DSR bitumen sample was employed to measure the $|G^*_0|$ and δ_0 with the LAS start and end strain levels ranging from 0.1% and 0.5% (both less than 0.8%). The $|G^*_0|$ and δ_0 of the PAV-aged control bitumen, unaged and PAV-aged bio-oil modified bitumen, and unaged and PAV-aged LDPE modified bitumen were obtained using the same method.

b) Frequency sweep and fatigue tests to determine viscoelasticity and fatigue properties

Frequency sweep tests with strain level of 0.5% using the DSR were conducted at temperature sequence of 70°C, 60°C, 50°C, 40°C, 30°C, 20°C, and 10°C, and in a frequency range from 0.1Hz to 25Hz. It should be stressed that there is no fatigue damage introduced in all these scenarios. The dynamic shear moduli and phase angles were obtained at the above temperatures and frequencies, and master curves of the dynamic shear modulus and phase angle can be accurately constructed [46]. Then, by using the interconversion equations for linear viscoelastic material [47], shear relaxation modulus can be accurately calculated, where the model parameter G_1 and m' can be determined.

A strain-controlled fatigue test based on time sweep procedure of the DSR was employed to characterise fatigue cracking performance of the bitumen (10Hz, 20°C). The time sweep test was conducted using sinusoidal loading with a rotational amplitude (i.e., θ) of 0.025 rad to achieve the target strain level of 5% at the edge of the bitumen sample. The reason of the selection of 5% target strain level is that 5% strain level was well controlled for the waste-derived bitumen in the full time sweep loading history, which yielded reliable test results. The schematic plot of the loading sequences employed in the experiments can be found in **Figure 4**.

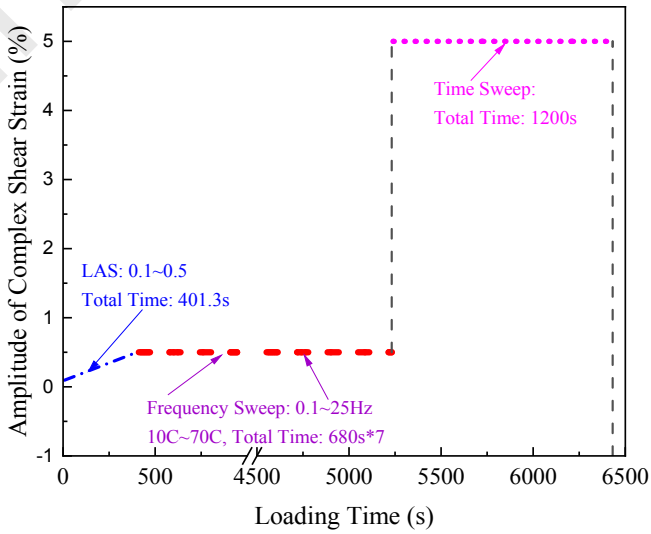

Figure 4. Loading sequences of the LAS, frequency sweep testing and fatigue tests

The reason why the strain-controlled test rather than the stress-controlled one was employed is that the stress-controlled test introduces an unstable or unmeasurable crack growth at some point of the test, which makes the evaluation of fatigue cracking unreliable. In the strain-controlled test, both the initiation and propagation of fatigue cracking are more stable, and the experimental results are well replicated. Therefore, the strain-controlled mode instead of the stress-controlled one were selected to characterise the fatigue performances of the bitumen.

c) Contact angle tests to determine surface energy

Sessile drop method (using Attension Theta Flex optical tensiometer) was adopted to measure the contact angles of the bitumen surfaces with different probe liquids. The contact angle results were then used to determine surface energy components using **Equation (9)**. There are two types of dynamic contact angles (i.e., advancing, and receding contact angles) can be measured by the mode of automatic dynamic contact angle built-in the tensiometer. Lytton et al. [48] stated that the surface energy calculated from the advancing contact angle contributed to crack surface wetting and was related to the healing process; the receding contact angle was associated with the de-wetting thus linked to the crack opening process. For cracking purpose, this study used the receding contact angles to determine the surface energies of the materials.

Automatic dynamic contact angle experiments are conducted to obtain the receding contact angles between the bitumen samples and five preselected probe liquids (i.e., Ethylene glycol, Water, Formamide, Glycerol, and Diiodomethane) with known surface energy components. For each liquid, three clean and dry microscope slides coated with the bitumen were utilised to reduce the variation of contact angle measurements. An automatic dispenser with a gauge needle and an adapter containing different probe liquids was utilised herein. The adapter was mounted to the dispenser and the needle was connected to the adapter. When the sample for the experiment was in place of the tensiometer, key configurations of built-in software (i.e., OneAttension software) were set up immediately, including the creation of the user level, selection of the experimental mode (i.e., automatic dynamic contact angle), completion of the recipe (critical parameters of the experiment can be transmitted to the computer). Once all the above controls have been set up, the experiment can be started and continued until its completion.

There are two options (i.e., tilting cradle and thin needle method) available to obtain the dynamic contact angles with the tensiometer. Tilting method was used herein to measure the receding contact angle, which mainly includes the following steps: 1) A droplet of the probe liquid is placed on the bitumen sample surface and tilting starts; 2) Once the droplet starts moving on the bitumen sample surface, the receding contact angle have been reached, and the roll-off angle of the surface is also detected; 3) After setting the baseline to the bitumen surface, contact angles can be imaged directly by the image recording system of the tensiometer. The built-in software of the test equipment automatically recognises and calculates the receding contact angle between the selected probe liquid and the bitumen.

4. Results and Discussion

4.1 Improvements of Cracking Performance of Unaged Bitumen Modified by Bio-oil or LDPE

Figure 5 shows the evolution of crack length determined by **Equation (1)** for the unaged bitumen, which can be divided into three parts, including crack initiation phase, plateau phase and propagation phase. The behaviour of the crack initiation phase is governed by the modified Griffith criterion shown in **Equation (8)**, and the propagation phase is controlled by

the modified Paris' law shown in **Equation (2)**. In the plateau phase, cracks grow slowly with load cycle, which is believed to result from the restructure of the microstructure of the unaged bitumen after the crack initiation, particularly for the rearrangement of the lightweight components in the bitumen (e.g., saturates and aromatic) and this delays the growth of the cracks. It is expected this plateau phase is minimised or will disappear when the bitumen becomes aged due to the loss of the lightweight component during ageing, which will be discussed later.

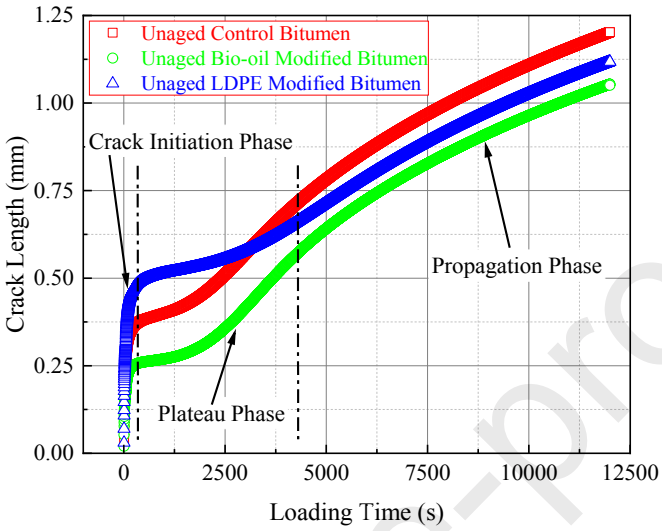

Figure 5. Evolutions of crack lengths of the unaged control bitumen, bio-oil modified bitumen, and LDPE modified bitumen

Figure 5 also shows that the bio-oil substantially reduces the crack length thus enhances the crack resistance of the unaged bitumen in the whole loading times; and this is due to that the bio-oil contains more saturates with light molecules [13], rejuvenating the bitumen and increasing the cracking resistance of the material. The LDPE-modified bitumen has more severe cracking in the first 425 load cycles than the control bitumen, and after that the LDPE gradually inhibits the crack growth, leading to a lower crack growth in the unaged bitumen. The fundamental reasons behind this observation is that the short molecular chain of the LDPE melted in the bitumen can effectively increase the lightweight components and absorb the polar and interactive asphaltenes of the unaged control bitumen [49], which helps to form a network structure with a continuous polymer phase and strengthen the anti-crack performance in the plateau phase. This absorption and network formation may take some time thus will not reduce the crack growth until the plateau phase is finished and the propagation starts.

The above observations can be verified by theories of crack initiation (i.e., **Equation (8)**), and propagation (i.e., **Equations (2)~(5)**). The surface energy calculated from the receding contact angles of the unaged bitumen can be obtained by the following two steps: 1) measure the receding contact angles between the bitumen and five different probe liquids; and 2) employ a least square method [50] to optimise the value of the surface energy of the unaged bitumen based on **Equations (9)** and **(10)**. The calculated surface energy, dynamic shear modulus and phase angle of the unaged bitumen are summarised in **Table 2**.

Table 2. Receding surface energy* Γ_f, dynamic shear modulus $|G^*_0|$ and phase angle δ_0 of the unaged bitumen

Control bitumen	Γ_f (mJ/m^2)	$\lvert G^*_0\rvert$ (kPa)	δ_0 (°)

	25.3	6123.4	55.9
Bio-modified bitumen	23.3	2448.1	63.4
LDPE-modified bitumen	33.5	10744.7	47.9

* Receding surface energy implies that this surface energy is calculated from receding contact angle test.

After substituting the receding surface energy, dynamic shear modulus of the unaged bitumen and edge flow crack length (i.e., 0.3898mm, 0.2660mm, and 0.5134mm, respectively, for the unaged control bitumen, bio-oil modified bitumen, and LDPE modified bitumen) into **Equation (8)**, the critical strain levels $\gamma_{0initiate}$ are determined as 0.778%, 0.803%, and 0.650% for the unaged control bitumen, bio-oil modified bitumen, and LDPE-modified bitumen, respectively. Details of calculation of edge flow crack length can be found in the authors' previous work [43]. Hence, it is noticed that the bio-oil can delay, and the LDPE brings forward the crack initiation of the unaged bitumen, respectively. Furthermore, it is noteworthy that the bio-oil can effectively decrease and LDEP increases the crack length of the bitumen at the end of crack initiation phase. **Equation (8)** also shows that $\gamma_{0initiate}$ is composed of two parts, which are induced by damaged parameter (i.e., edge flow crack length), and undamaged parameters (i.e., material modulus and surface energy), respectively. The authors find that the above damaged parameter contributes to 62.6%, 41.4%, and 98.8% of the critical strain levels $\gamma_{0initiate}$ for the unaged control bitumen, bio-oil modified bitumen, and LDPE modified bitumen, respectively. This means the LDPE modified bitumen is most affected by the edge flow.

In the crack propagation phase, crack growth rate is determined using parameters of ΔJ_R, A, and n. The crack parameters A and n are determined by **Equations (4)** and **(5)**, where the testing results from the frequency sweep test within the linear viscoelastic range (10Hz, 10~70°C) and LAS test (0.1%~0.5%, 20°C) were used. Specifically, the shear relaxation modulus parameters m' and G_1 are determined using following steps: 1) Constructions of the master curves of shear dynamic modulus and phase angle of the unaged bitumen at the reference temperature of 20°C using the time-temperature superposition principle (e.g., WLF equation); 2) Calculation of Prony model parameters of shear relaxation modulus by the collocation method [47] and the least squared regression minimization [51]; 3) Interconversion between Prony model parameters and power model parameters of shear relaxation modulus (i.e., $G(t) = G_1 t^{-m'}$). **Table 3** summaries the values of shear relaxation modulus parameters (m', G_1) and shear strength (τ_m) of the unaged control bitumen, bio-oil modified bitumen, and LDPE modified bitumen.

Table 3. Shear relaxation modulus parameters (m', G_1) and shear strength (τ_m) of the unaged bitumen

	m'	G_1 (kPa)	τ_m (kPa)
Control bitumen	0.7978	2398.8	290.4
Bio-modified bitumen	0.8290	480.2	161.7
LDPE-modified bitumen	0.7154	3680.2	998.1

Substituting the above-mentioned parameters into **Equations (3)~(5)**, ΔJ_R shown in **Figure 6** and crack parameters A and n can be accurately calculated for three different types of unaged bitumen. **Figure 6** clearly shows that the ΔJ_R of the unaged bitumen decreases with the load cycle, which is reasonable since a strain-controlled time sweep fatigue test was used and the energy dissipated for cracking was reducing with loading cycle. The LDPE increases and bio-oil reduces ΔJ_R of the unaged bitumen, which implies that, when adding to the bitumen, LDPE and bio-oil make the dissipated energy for cracking quicker and slower, respectively.

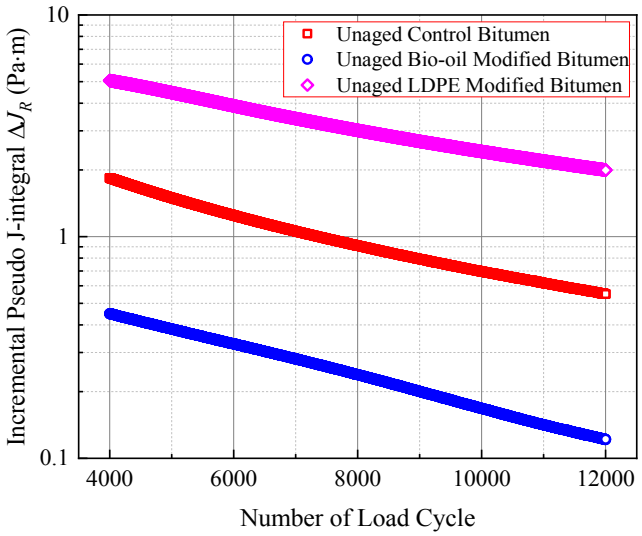

Figure 6. Evolutions of incremental pseudo *J*-integral (ΔJ_R) of the unaged control bitumen, bio-oil modified bitumen, and LDPE modified bitumen

Then, the crack propagation can be predicted using the modified Paris' law in **Equation (2)** for the unaged control bitumen, bio-oil modified bitumen, and LDPE modified bitumen. The predicted crack growth rates are compared with those directly measured from **Figure 5** and shown in **Figure 7**. It demonstrates that the measured values agree well with the predicted ones (R^2 is greater than 0.9 for the three bitumen). It can be found in **Figure 7** that neither the bio-oil nor the LDPE can effectively change the crack growth rate of the unaged bitumen, although they can substantially alter the crack initiation of the control bitumen as shown in **Figure 5**. Hence, it can be concluded that both bio-oil and LDPE can affect the crack initiation of the bitumen, but not the crack propagation. It is the bitumen rather than the additives such as bio-oil or LDPE that fundamentally determine the rate of the crack propagation. It is worthy to note that the inclusion of bio-oil or LDPE in bitumen can change the values of ΔJ_R, A, and n, but the crack growth rates remain unchanged.

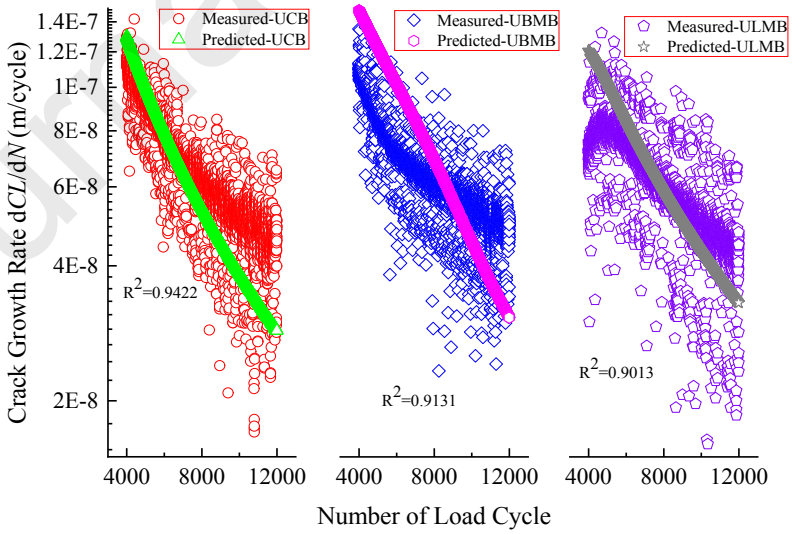

Figure 7. Comparisons of the crack growth rate predicted using Paris' law and measured from the crack length for three unaged bitumen materials (UCB, UBMB, and ULMB stand for the unaged control bitumen, unaged bio-oil modified bitumen, and unaged LDPE modified bitumen, respectively)

4.2 Comparisons of Cracking Performance Between PAV-aged Control Bitumen, Bio-oil Modified Bitumen, and LDPE Modified Bitumen

Figure 8 shows that the curves of crack evolution determined from **Equation (1)** for the PAV-aged control bitumen and bio-oil modified bitumen overlap with each other. This results from that the bio-oil modified bitumen loses most of the bio-oil additives during the ageing process, thus the remained bio-oil modified bitumen after ageing shows similar or identical behavior as the PAV-aged control bitumen. The PAV-aged LDPE modified bitumen has much more severe cracking than the ones of two other PAV-aged bitumen. The factors contributing to this phenomena mainly include 1) acceleration of the crack initiation due to the inclusion of the LDPE, and 2) disappearance of the plateau phase because of the loss of light fractions (e.g., saturates and aromatic) caused by the ageing process.

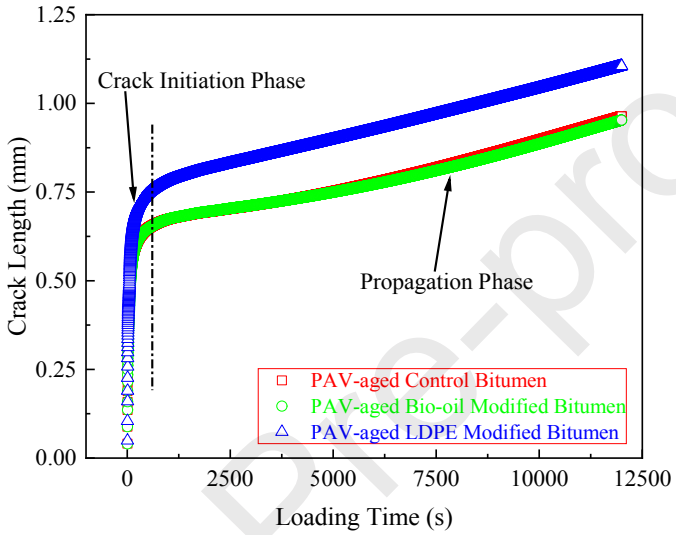

Figure 8. Evolutions of crack length of the PAV-aged control bitumen, bio-oil modified bitumen, and LDEP modified bitumen

It is well documented [52, 53] that the chemical changes of the bitumen after the PAV ageing include the formation of new functional groups (e.g., carbonyls and sulfoxides), transformation of generic fractions and changes in molecular weight (e.g., decreases of saturates and aromatics and increases of resins and asphaltenes). Due to those ageing-induced chemical changes, the PAV-aged bitumen becomes stiffer and more susceptible to damage, which lead to severe crack growth in the PAV-aged bitumen even at the crack initiation phase as observed in **Figure 8**. This can be demonstrated by the comparisons of crack lengths at the initiation between the aged and unaged bitumen. **Figure 8** shows that the crack lengths of the PAV-aged control bitumen, bio-oil modified bitumen, and LDPE modified bitumen at the end of crack initiation phase are 0.6651mm, 0.6651mm, and 0.7693mm, respectively. In comparison, **Figures 5** shows that the crack lengths for the three bitumen without ageing are 0.3706mm, 0.2558mm, and 0.4824mm, respectively.

The disappearance of the plateau phase is due to the following reasons: 1) the increased dynamic modulus of the bitumen after PAV ageing makes the dissipated strain energy for cracking (that is proportional to the square of the dynamic modulus of the bitumen) accumulate more quickly, which accelerates the crack initiation phase; 2) the reductions of saturates and aromatics and the increases of resins and asphaltenes in the PAV-aged bitumen substantially reduce its ability to reconstruct the microstructure and redistribute the accumulated strain energy when the crack initiation is introduced. Therefore, the plateau phase of the crack evolution is no longer observable after the PAV ageing, and the crack

damage of the bitumen after the PAV ageing rapidly steps into the propagation phase.

Models of crack initiation (i.e., **Equations (8)**) and propagation (i.e., **Equations (2)~(5)**) are also employed herein to verify the crack growth in the PAV modified bitumen shown in **Figure 8**. First of all, the material properties for the PAV-aged bitumen were obtained using the methods explained in Section 3.3 and the results are shown in **Table 4** including the receding surface energy, dynamic shear modulus and phase angle of the PAV-aged bitumen.

Table 4. Receding Surface energy Γ_f, dynamic shear modulus $|G^*_0|$ and phase angle δ_0 of the PAV-aged bitumen

	Γ_f (mJ/m^2)	$\lvert G^*_0 \rvert$ (kPa)	δ_0 (°)
Control bitumen	34.35	15681.7	39.2
Bio-modified bitumen	37.90	14367.3	40.2
LDPE-modified bitumen	48.71	27070.8	34.3

Second, the edge flow crack lengths (i.e., CL_0) for the PAV-aged control bitumen, bio-oil modified bitumen, and LDPE modified bitumen are 0.6977mm, 0.6988mm, and 0.8328mm, respectively, which are substantially longer than the ones of the corresponding unaged bitumen shown in Section 4.1. Details of calculation of edge flow crack length can be found in the authors' previous work [43].

Then, following the same methods in Section 4.1, the value of $\gamma_{0initiate}$ for the PAV-aged bitumen can be calculated by substituting the receding surface energy, dynamic shear modulus and edge flow crack length of the bitumen into **Equation (8)**. The calculated $\gamma_{0initiate}$ for the PAV-aged control bitumen, bio-oil modified bitumen, and LDPE modified bitumen are 0.8765%, 0.8781%, and 1.0451%, respectively. Compared with the $\gamma_{0initiate}$ of the unaged bitumen, the ageing processes increase the $\gamma_{0initiate}$ for 12.7%, 9.4%, and 60.8% for the control bitumen, bio-oil bitumen, and LDPE modified bitumen, respectively. It should be noted that although the ageing processes delay the crack initiation for the PAV-aged LDPE modified bitumen as showed by the higher critical strain level (1.0451%), they also produce much longer crack length (0.8328mm) when the crack is initiated. Since the crack evolution remains similar between the three bitumen materials, the end-of-life crack length becomes dependent of the initial crack length. Thus, the LDPE modified bitumen shows the highest crack length after the fatigue loading.

In the crack propagation phase of the bitumen after PAV ageing shown in **Figure 8**, there is very little observable influence of the LDPE on the crack growth rate of the PAV-aged bitumen, which is the same as that shown in the unaged scenario. Hence, it can be concluded that the crack propagation rate is mainly governed by the bitumen itself and almost not affected by the additives like bio-oil or LDPE in the bitumen. Additionally, Paris' law shown in **Equations (2)~(5)** are employed to quantify how the crack parameters of the PAV-aged bitumen to affect the crack propagation. **Table 5** presents the values of m', G_1, and τ_m of the PAV-aged control bitumen, bio-oil modified bitumen, and LDPE modified bitumen.

Table 5. Shear relaxation modulus parameters (m', G_1) and shear strength (τ_m) of the PAV-aged bitumen

	m'	G_1 (kPa)	τ_m (kPa)
Control bitumen	0.7064	12251.3	1090.4
Bio-modified bitumen	0.6598	12198.3	1270.0

LDPE-modified bitumen	0.6399	21656.6	1783.9

As completed in Section 4.1, the incremental pseudo *J*-integral (i.e., ΔJ_R) shown in **Figure 9** and crack parameters (i.e., *A* and *n* discussed later) of the PAV-aged bitumen are calculated, based on which crack propagation of the bitumen after PAV ageing is predicted and compared with the one directly measured (i.e., measured values) from **Figure 8**. Details are presented in **Figure 10**.

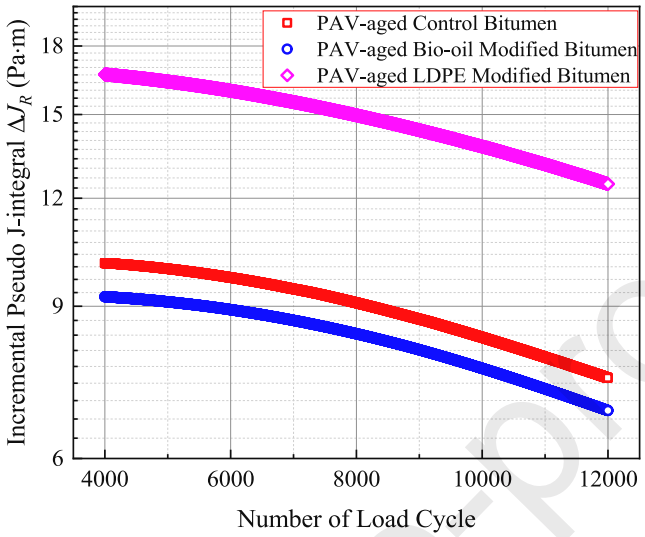

Figure 9. Evolutions of incremental pseudo *J*-integral (ΔJ_R) of the PAV-aged control bitumen, bio-oil modified bitumen, and LDPE modified bitumen

Figure 9 shows that the ΔJ_R of the PAV-aged bitumen decreases with the load cycle. The LDPE increases and bio-oil slightly reduces the ΔJ_R of the PAV-aged bitumen, which implies that LDPE makes the energy dissipation for cracking much quicker than the PAV-aged control bitumen. In comparison, the bio-oil make this energy dissipation a bit slower. A reminder is that most of bio-oil has been evaporated during the ageing processes thus the PAV-aged bio-oil modified bitumen did not show obvious difference from the PAV-aged control bitumen. Compared with the unaged bitumen presented in **Figure 6**, **Figure 9** shows that the ageing significantly increases the ΔJ_R of all three types of the bitumen. This observation indicates that the ageing makes the energy dissipation for cracking much quicker in the aged bitumen than that in the unaged bitumen. This is expected as the critical reason why the aged bitumen is more prone to cracking, no matter if the bitumen is unmodified or modified ones.

It can be found in **Figure 10** that the crack growth rates predicted by **Equations (3)~(5)** are consistent well with the measured ones. **Equations (3)~(5)** also recall the authors that cracking related parameters of *A* and *n* are the functions of the fundamental material constants shown in **Equations (4)** and **(5)**. These fundamental constants include receding surface energy, shear strength and shear modulus and phase angle of the bitumen. The effects of external load and damage history on the crack growth rate are reflected by the ΔJ_R, which is explicitly related with the amplitude of loading using the rotational angle θ, and the residual uncracked radius of the DSR sample r_E (an indication of the current crack length). In addition, it is again noted that the inclusion of bio-oil or LDPE in bitumen can change the values of ΔJ_R, *A*, and *n* (shown in **Figure 11**) of the PAV-aged bitumen; however, the crack growth rates of the bitumen modified by the bio-oils or LDPE still kept the same to the control bitumen. **Figure 11** presents the values of *A* and *n* of the unaged and PAV-aged

bitumen.

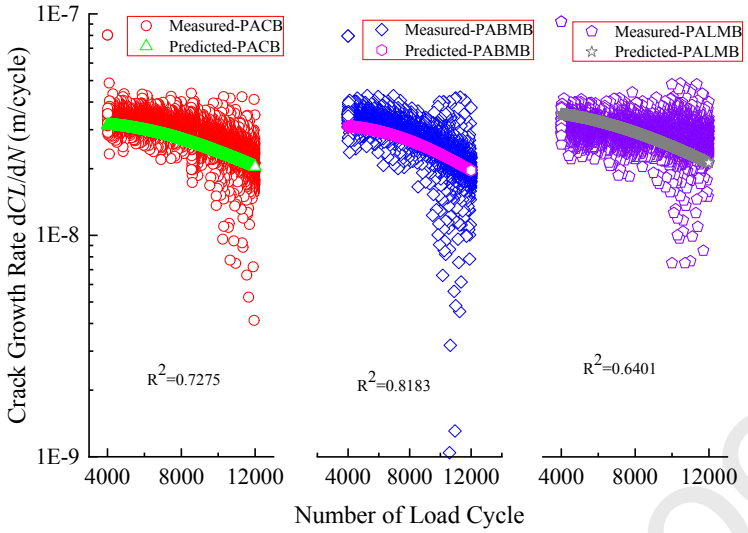

Figure 10. Comparisons of the crack growth rate predicted using Paris' law and measured from the crack length for three PAV-aged bitumen materials (PACB, PABMB, and PALMB signify the PAV-aged control bitumen, PAV-aged bio-oil modified bitumen, and PAV-aged LDPE modified bitumen, respectively)

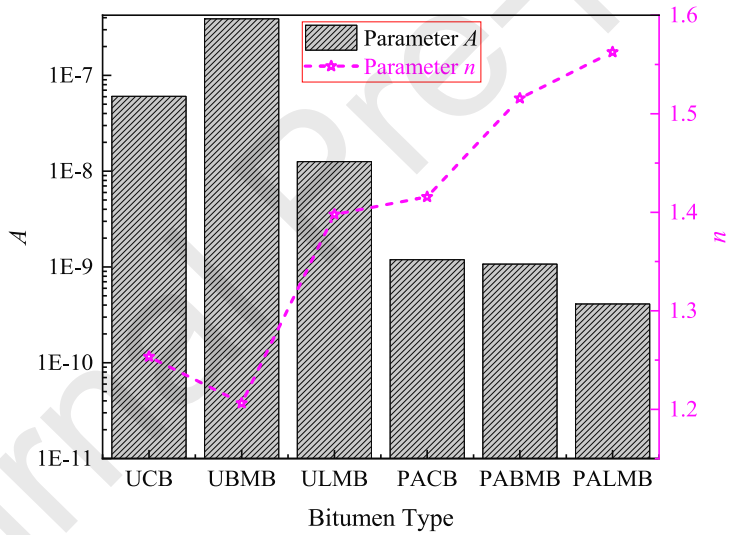

Figure 11. Paris' law parameters *A* and *n* for modelling fatigue cracking in the bitumen (UCB, UBMB, ULMB, PACB, PABMB, and PALMB stand for unaged control bitumen, unaged bio-oil modified bitumen, unaged LDPE modified bitumen, PAV-aged control bitumen, PAV-aged bio-oil modified bitumen, and PAV-aged LDPE modified bitumen, respectively)

Figure 11 shows that the bio-oil considerably increases the value of *A*, and markedly reduces the value of *n* of the unaged control bitumen. The LDPE can decrease the value of *A*, and effectively increase the value of *n* of the unaged control bitumen. After ageing, the value of *A* is observed to reduce, and the value of *n* is found to increase, respectively. Compared with the valves of *A* and *n* of the PAV-aged control and bio-oil modified bitumen (most of the bio-oil has been evaporated), the PAV-aged LDPE modified bitumen is found to have much higher value of *n* and lower value of *A*. Therefore, synthetically taking the information released by **Figures 7**, **10**, and **11**, it can be drawn a conclusion that the crack growth rate of

the bitumen increases with material parameter A and decreases with material parameter n.

5. Summary and Conclusions

This paper characterised the cracking performances of the unaged and PAV-aged waste-derived bitumen (i.e., bio-oil modified bitumen, and LDPE modified bitumen) based on crack length. The bio-oil modified bitumen was fabricated using bio-oil pyrolysed from organic fraction of municipal solid waste and mixed with a control bitumen (X70) at a concentration of 5wt.%. The LDPE modified bitumen was fabricated by blending waste plastics (6wt.% LDPE) with the control bitumen at 180°C using a high shear mixer at 900 rotation per minute. Modified Paris' law and Griffith criterion were employed to model the crack propagation and initiation of the unaged and PAV-aged bitumen. Material parameters (e.g., dynamic modulus, surface energy, and shear strength) of the unaged and the PAV-aged bitumen used in the cracking models were calibrated using linear amplitude sweep test (10Hz and 20°C), frequency sweep test (10Hz, 10 to 70°C), and strain-controlled time sweep test (10Hz and 20°C) with a damage strain level of 5%. Receding contact angles between the unaged or PAV-aged bitumen and the selected probe liquids were measured by the tilting method based on sessile drop tensiometer. The main findings and conclusions of this paper are summarised as follows:

(1) The crack evolution of the unaged bitumen can be divided into three phases, including crack initiation phase governed by the modified Griffith criterion, plateau phase, and propagation phase controlled by the modified Paris' law. The plateau phase is believed to result from the restructure of the bitumen microstructure after the crack initiation, particularly from the rearrangement of the lightweight components in the bitumen (e.g., saturates and aromatic), and this delays the growth of the cracks.

(2) The bio-oil delays and the LDPE brings forward fatigue crack initiation of the unaged bitumen, and the bitumen itself dominates the crack propagation process. The LDPE inhibits the crack growth rate of the unaged bitumen in the plateau phase. In contrast, the effect of the bio-oil on the crack growth rate of the unaged bitumen in the plateau phase can be neglected.

(3) After PAV ageing the plateau phase of the crack evolution no longer exists, and the crack damage in the PAV-aged bitumen rapidly steps into the propagation phase after the crack initiation phase. PAV ageing can make the bitumen more prone to crack mainly on account of severe fatigue crack appeared in the phase of crack initiation.

(4) The bio-oil modified bitumen loses most of the modifier due to the evaporation of the bio-oils during the ageing process. The PAV-aged LDPE modified bitumen has more severe cracking than those of the PAV-aged control bitumen or bio-oil modified bitumen. The LDPE leads to higher crack length in the PAV-aged bitumen at the crack initiation phase; however, it has little influence on the crack growth rate of the PAV-aged bitumen during the propagation phase.

Conflict of interest

The authors declared that there is no conflict of interest.

Acknowledgements

The authors would like to acknowledge the financial support from Marie Skłodowska-Curie Individual Fellowships of EU under EU's H2020 programme (Grant No. 789551), the National Nature Science Foundation of China (Grant No. 51978229), AIMR Seedcorn Grant from Aston University of Unite Kingdom (Grant No. 201901), and China Postdoctoral

Science Foundation funded Project (Grant No. 2015M571928).

Appendix

Crack Initiation of The Bitumen in The DSR Test Based on Modified Griffith Criterion

To mitigate the viscous effect of the bitumen, the concept of pseudo-strain γ^R was proposed by Schapery [38], and its definition can be presented by **Equation (A.1)**:

$$\gamma^R(t)=\frac{1}{G_R}\int_{0^-}^{t}G(t-s)\dot{\gamma}(s)\,ds \tag{A.1}$$

Where, $\gamma(s)$ is the measured total strain; and s is the time history before the current time t. According to **Equation (A.1)**, the pseudo-strain γ_d^R at the damaged condition in a strain-controlled DSR test can be presented as follows:

$$\gamma_d^R(t)=\frac{|G_0^*|}{G_R}\gamma_d\sin(\omega t+\delta_0)=\frac{|G_0^*|}{G_R}\frac{\theta}{h}r\sin(\omega t+\delta_0)\quad \text{with } 0\le r\le r_0 \tag{A.2}$$

Where, γ_d^R is the shear strain at the damaged condition; ω is the loading frequency.

The recovered pseudo strain energy *RPSE* at the N^{th} load cycle can be defined by **Equation (A.3)**:

$$RPSE=\frac{1}{2}\tau_0\gamma_{d0}^R=\frac{1}{2}\frac{|G_0^*|^2\theta^2}{G_Rh^2}r^2 \tag{A.3}$$

Where, τ_0, equalling to $\frac{|G_0^*|\theta}{h}r$, is the amplitude of the fatigue shear stress during the DSR test; γ_{d0}^R is the amplitude of the shear strain at the damaged condition shown in **Equation (A.2)**.

Figure A presents the schematic side view of cylindrical bitumen sample in the DSR test. It is straightforward to calculate the first part W_1^R of **Equation (7)** by substituting **Equation (A.3)** into it:

$$W_1^R=\int_0^{r_0}RPSE\cdot(2\pi rh)\,dr=\frac{\pi}{4}\frac{\left(|G_0^*|\theta\right)^2}{G_Rh}r_0^4 \tag{A.4}$$

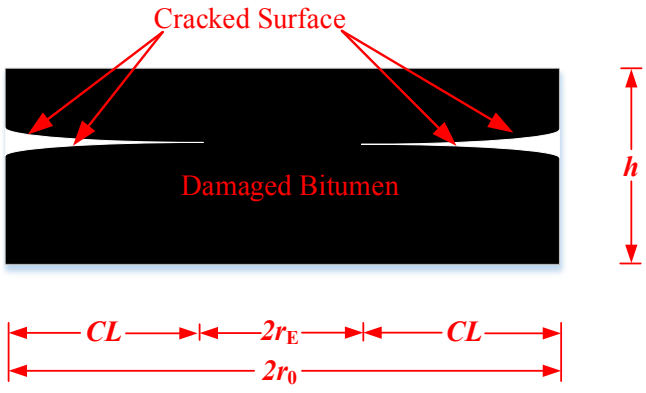

Figure A. Schematic side view of cylindrical bitumen sample under rotational fatigue load of the DSR test

The second part W_2^R of **Equation (7)** can be calculated as follows:

$$W_2^R = \int_{r_E}^{r_0} RPSE \cdot (2\pi rh)\, dr = \frac{\pi}{4} \frac{\left(\left|G_0^*\right|\theta\right)^2}{G_R h} \left[r_0^4 - \left(r_0 - CL\right)^4 \right] \tag{A.5}$$

As shown in **Figure A**, the crack surface areas *C.S.A* can be calculated by **Equation (A.6)**:

$$C.S.A = 2\left(\pi r_0^2 - \pi r_E^2\right) = 2\pi\left(-CL^2 + 2r_0 CL\right) \tag{A.6}$$

Substituting **Equations (A.4-A.6)** to **Equation (7)**, the total pseudo strain energy W^R can be explicitly obtained. Combing the calculated W^R and modified Griffith criterion shown in **Equation (6)**, then one has:

$$r_0 = CL_0 + \frac{2h}{\left|G_0^*\right|\theta}\left(\frac{G_R}{h}\Gamma_f\right)^{1/2} \tag{A.7}$$

Substituting the relationship between $\gamma_{0initiate}$ and r_0 (i.e., $\gamma_{0initiate}=\theta r_0/h$) into **Equation (A.7)**, **Equation (8)** is obtained.

References

[1] M. Hafez, K. Ksaibati, R. Atadero, Developing a methodology to evaluate the effectiveness of pavement treatments applied to low-volume paved roads, International Journal of Pavement Engineering, 20 (2019) 894-904.
[2] L.L. Li, X.M. Huang, D. Han, M.S. Dong, D.Y. Zhu, Investigation of rutting behavior of asphalt pavement in long and steep section of mountainous highway with overloading, Construction and Building Materials, 93 (2015) 635-643.
[3] X.Y. Liu, J.L. Li, G. Tzimiris, T. Scarpas, Modelling of five-point bending beam test for asphalt surfacing system on orthotropic steel deck bridges, International Journal of Pavement Engineering.
[4] K. Kumar, J. Kozak, L. Hundal, A. Cox, H. Zhang, T. Granato, In-situ infiltration performance of different permeable pavements in a employee used parking lot - A four-year study, Journal of Environmental Management, 167 (2016) 8-14.
[5] G. White, Quantifying the impact of reclaimed asphalt pavement on airport asphalt surfaces, Construction and Building Materials, 197 (2019) 757-765.
[6] M.M.M. Ali, H.Y. Zhao, Z.Y. Li, N.N.M. Maglas, Concentrations of TENORMs in the petroleum industry and their environmental and health effects, Rsc Advances, 9 (2019) 39201-39229.
[7] S.B. Kulkarni, M.S. Ranadive, Modified Cutback as Tack Coat by Application of Pyro-Oil Obtained from Municipal Plastic Waste: Experimental Approach, Journal of Materials in Civil Engineering, 32 (2020).
[8] M. Nouali, E. Ghorbel, Z. Derriche, Phase separation and thermal degradation of plastic bag waste modified bitumen during high temperature storage, Construction and Building Materials, 239 (2020).
[9] S.A. Abd Kader, R.P. Jaya, H. Yaacob, M.R. Hainin, N.A. Hassan, M.H.W. Ibrahim, A.A. Mohamed, Ichwana, Stability and Volumetric Properties of Asphalt Mixture Containing Waste Plastic, in: M.J. Zainorizuan, L.Y. Yong, L. Siang, O.M. Hanifi, R.S. Nazahiyah, A.M.

Shalahuddin (Eds.) International Symposium on Civil and Environmental Engineering 2016, 2017.
[10] N.M. Tuan, Effect of Polyethylene Terephthalate (PET) from Plastic Waste on Strength of Hot Mix Asphalt Concrete in Southern Vietnam, 2016.
[11] Z. Leng, A. Sreeram, R.K. Padhan, Z.F. Tan, Value-added application of waste PET based additives in bituminous mixtures containing high percentage of reclaimed asphalt pavement (RAP), Journal of Cleaner Production, 196 (2018) 615-625.
[12] S. Angelone, M.C. Casaux, M. Borghi, F.O. Martinez, Green pavements: reuse of plastic waste in asphalt mixtures, Materials and Structures, 49 (2016) 1655-1665.
[13] Y. Yang, Y.Q. Zhang, E. Omairey, J.M. Cai, F. Gu, A.V. Bridgwater, Intermediate pyrolysis of organic fraction of municipal solid waste and rheological study of the pyrolysis oil for potential use as bio-bitumen, Journal of Cleaner Production, 187 (2018) 390-399.
[14] Z.G. Feng, W.Y. Rao, C. Chen, B. Tian, X.J. Li, P.L. Li, Q.L. Guo, Performance evaluation of bitumen modified with pyrolysis carbon black made from waste tyres, Construction and Building Materials, 111 (2016) 495-501.
[15] Z.M. Si, D.N. Little, R.L. Lytton, Characterization of microdamage and healing of asphalt concrete mixtures, Journal of Materials in Civil Engineering, 14 (2002) 461-470.
[16] X.D. Hu, L.F. Walubita, Modelling Tensile Strain Response in Asphalt Pavements Bottom-up and/or Top-down Fatigue Crack Initiation, Road Materials and Pavement Design, 10 (2009) 125-154.
[17] H.D. Kuai, H.J. Lee, J.H. Lee, S. Mun, Fatigue Crack Propagation Model of Asphalt Concrete Based on Viscoelastic Fracture Mechanics, Transportation Research Record, (2010) 11-18.
[18] M.T. Nguyen, H.J. Lee, J. Baek, J.S. Moon, A New Fatigue Failure Criterion Based on Crack Width of Asphalt Concrete Under Indirect Tensile Mode of Loading, Journal of Testing and Evaluation, 44 (2016) 55-66.
[19] S.M. Damadi, A. Edrisi, M. Fakhri, S. Rezaei, M.W. Khordehbinan, Fatigue Analysis of Bitumen Modified with Composite of Nano-SiO2 and Styrene Butadiene Styrene Polymer, Frat. Integrita Strut., (2020) 202-209.
[20] M. Ameri, A. Mansourkhaki, D. Daryaee, Evaluation of fatigue behavior of high reclaimed asphalt binder mixes modified with rejuvenator and softer bitumen, Construction and Building Materials, 191 (2018) 702-712.
[21] (!!! INVALID CITATION !!! [21, 22]).
[22] H. Ziari, R. Babagoli, A. Akbari, Investigation of fatigue and rutting performance of hot mix asphalt mixtures prepared by bentonite-modified bitumen, Road Materials and Pavement Design, 16 (2015) 101-118.
[23] G. Liu, M. van de Ven, S.P. Wu, J.Y. Yu, A. Molenaar, Influence of organo-montmorillonites on fatigue properties of bitumen and mortar, International Journal of Fatigue, 33 (2011) 1574-1582.
[24] D.A. Anderson, T.W. Kennedy, Development of SHRP binder specification (with discussion), Journal of the Association of Asphalt Paving Technologists, 62 (1993).
[25] J.P. Planche, D.A. Anderson, G. Gauthier, Y.M. Le Hir, D. Martin, Evaluation of fatigue properties of bituminous binders, Materials and Structures, 37 (2004) 356-359.
[26] H.U. Bahia, H. Zhai, M. Zeng, Y. Hu, P. Turner, Development of binder specification parameters based on characterization of damage behavior (with discussion), Journal of the Association of Asphalt Paving Technologists, 70 (2001).
[27] S. Shen, S.H. Carpenter, Application of the dissipated energy concept in fatigue endurance limit testing, Transportation research record, 1929 (2005) 165-173.
[28] F. Zhou, W. Mogawer, H. Li, A. Andriescu, A. Copeland, Evaluation of fatigue tests for characterizing asphalt binders, Journal of Materials in Civil Engineering, 25 (2013) 610-617.

[29] D.A. Anderson, Y.M. Le Hir, M.O. Marasteanu, J.-P. Planche, D. Martin, G. Gauthier, Evaluation of fatigue criteria for asphalt binders, Transportation Research Record, 1766 (2001) 48-56.
[30] C. Hintz, R. Velasquez, C. Johnson, H. Bahia, Modification and validation of linear amplitude sweep test for binder fatigue specification, Transportation Research Record, 2207 (2011) 99-106.
[31] A. Pereira, R. Micaelo, L. Quaresma, M.T. Cidade, Evaluation of Different Methods for the Estimation of the Bitumen Fatigue Life with DSR Testing, in: F. Canestrari, M.N. Partl (Eds.) 8th Rilem International Symposium on Testing and Characterization of Sustainable and Innovative Bituminous Materials, Springer, Dordrecht, 2016, pp. 1017-1028.
[32] T.M. Ahmed, Fatigue performance of hot mix asphalt tested in controlled stress mode using dynamic shear rheometer, International Journal of Pavement Engineering, 20 (2019) 255-265.
[33] T.M. Ahmed, P.L. Green, H.A. Khalid, Predicting fatigue performance of hot mix asphalt using artificial neural networks, Road Materials and Pavement Design, 18 (2017) 141-154.
[34] A. Pereira, R. Micaelo, L. Quaresma, M.T. Cidade, Evaluation of different methods for the estimation of the bitumen fatigue life with DSR testing, in: 8th RILEM international symposium on testing and characterization of sustainable and innovative bituminous materials, Springer, 2016, pp. 1017-1028.
[35] Y. Zhang, Y. Gao, Predicting crack growth in viscoelastic bitumen under a rotational shear fatigue load, Road Materials and Pavement Design, (2019) 1-20.
[36] P. Paris, F. Erdogan, A critical analysis of crack propagation laws, (1963).
[37] R.L. Lytton, J. Uzan, E.G. Fernando, R. Roque, D. Hiltunen, S.M. Stoffels, Development and validation of performance prediction models and specifications for asphalt binders and paving mixes, Strategic Highway Research Program Washington, DC, 1993.
[38] R.A. Schapery, Correspondence principles and a generalizedJ integral for large deformation and fracture analysis of viscoelastic media, International Journal of Fracture, 25 (1984) 195-223.
[39] Y. Gao, L. Li, Y. Zhang, Modeling Crack Propagation in Bituminous Binders under a Rotational Shear Fatigue Load using Pseudo J-Integral Paris' Law, Transportation Research Record, (2019) 0361198119899151.
[40] Y. Zhang, R. Luo, R.L. Lytton, Characterizing permanent deformation and fracture of asphalt mixtures by using compressive dynamic modulus tests, Journal of Materials in Civil Engineering, 24 (2012) 898-906.
[41] R. Schapery, A method for predicting crack growth in nonhomogeneous viscoelastic media, International Journal of Fracture, 14 (1978) 293-309.
[42] A.A. Griffith, VI. The phenomena of rupture and flow in solids, Philosophical transactions of the royal society of london. Series A, containing papers of a mathematical or physical character, 221 (1921) 163-198.
[43] Y. Gao, L. Li, Y. Zhang, Modelling crack initiation in bituminous binders under a rotational shear fatigue load, International Journal of Fatigue, (2020) 105738.
[44] C.J. van Oss, Use of the combined Lifshitz–van der Waals and Lewis acid–base approaches in determining the apolar and polar contributions to surface and interfacial tensions and free energies, Journal of adhesion science and technology, 16 (2002) 669-677.
[45] AASHTO, Standard method of test for estimating damage tolerance of asphalt binders using the linear amplitude sweep, (2014).
[46] L. Li, W. Li, H. Wang, J. Zhao, Z. Wang, M. Dong, D. Han, Investigation of Prony series model related asphalt mixture properties under different confining pressures, Construction and Building Materials, 166 (2018) 147-157.

[47] S. Park, R. Schapery, Methods of interconversion between linear viscoelastic material functions. Part I—A numerical method based on Prony series, International journal of solids and structures, 36 (1999) 1653-1675.
[48] R.L. Lytton, E.A. Masad, C. Zollinger, R. Bulut, D.N. Little, Measurements of surface energy and its relationship to moisture damage, in: Application of Surface Energy Measurements to Evaluate Moisture Susceptibility of Asphalt and Aggregates, Texas Transportation Institute, The Texas A&M University System College Station, Texas 77843-3135, 2005, pp. 172.
[49] B. Singh, L. Kumar, M. Gupta, G. Chauhan, Polymer‐modified bitumen of recycled LDPE and maleated bitumen, Journal of applied polymer science, 127 (2013) 67-78.
[50] A.W. Hefer, A. Bhasin, D.N. Little, Bitumen surface energy characterization using a contact angle approach, Journal of Materials in Civil Engineering, 18 (2006) 759-767.
[51] L. Li, W. Li, Z. Wang, M. Dong, Y. Zhang, Characterizing stress-dependent complex and relaxation moduli of dense graded asphalt mixtures, Construction and Building Materials, 193 (2018) 55-63.
[52] X. Lu, U. Isacsson, Effect of ageing on bitumen chemistry and rheology, Construction and Building materials, 16 (2002) 15-22.
[53] G. Tarsi, A. Varveri, C. Lantieri, A. Scarpas, C. Sangiorgi, Effects of different aging methods on chemical and rheological properties of bitumen, Journal of Materials in Civil Engineering, 30 (2018) 04018009.

Graphical abstract

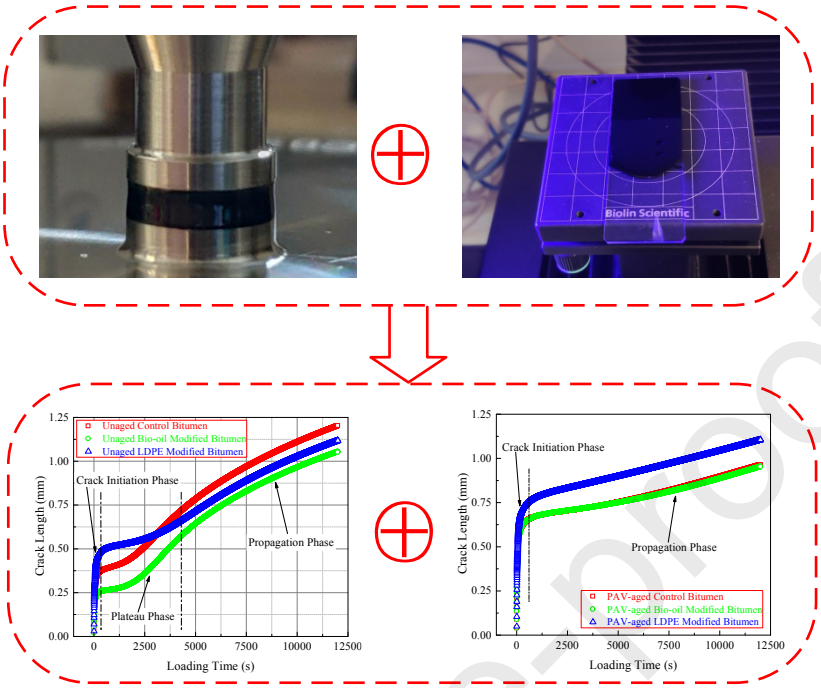

Highlights

- Fabricated two types of waste-derived bitumen
- Modelled crack growth using modified Griffith criterion and Paris' law
- Characterised fatigue cracking properties of waste-derived bitumen
- Analysed the effect of PAV ageing on fatigue cracking performances